

Received February 3, 2020, accepted March 9, 2020, date of current version March 19, 2020.

Digital Object Identifier 10.1109/ACCESS.2020.2980363

# Radar Signal Intra-Pulse Modulation Recognition Based on Convolutional Neural Network and Deep Q-Learning Network

ZHIYU QU<sup>ID</sup>, CHENFAN HOU<sup>ID</sup>, CHANGBO HOU<sup>ID</sup>, AND WENYANG WANG<sup>ID</sup>

College of Information and Communication Engineering, Harbin Engineering University, Harbin 150001, China

Corresponding author: Changbo Hou (houchangbo@hrbeu.edu.cn)

This work was supported in part by the National Natural Science Foundation of China under Grant 61671168 and Grant 61801143, in part by the Natural Science Foundation of Heilongjiang Province under Grant LH2019F005, and in part by the Fundamental Research Funds for the Central Universities under Grant 3072019CF0801 and Grant 3072019CFM0802.

**ABSTRACT** Intra-pulse modulation recognition of radar signals is an important part of modern electronic intelligence reconnaissance and electronic support systems. With the increasing density of radar signals, the analysis and processing of multi-component radar signals have become an urgent problem in the current radar reconnaissance system. In this paper, an intra-pulse modulation recognition approach for single-component and dual-component radar signals is proposed. First, in order to adapt to the time-frequency energy distribution characteristics of various radar signals, we propose to extract the time-frequency images (TFIs) of received signals by Cohen class time-frequency distribution (CTFD) with multiple kernel functions. Besides, the image processing methods are used to suppress noise and adjust the size and amplitude of the TFIs. Second, we design and pre-train a TFI feature extraction network for radar signals based on a convolutional neural network (CNN). Finally, to improve the probability of successful recognition (PSR) of the recognition system in the pulse overlapping environment, a multi-label classification network based on a deep Q-learning network (DQN) is explored. Besides, two sub-networks take TFIs based on special kernel functions as input and re-judge the recognition results of some specific signals to further enhance the recognition effect of the recognition system. The proposed approach can identify 8 kinds of random overlapping radar signals. The simulation results show that the overall PSR of dual-component radar signals and single-component radar signals can reach 94.83% and 94.43%, respectively, when the signal-to-noise ratio (SNR) is  $-6$  dB.

**INDEX TERMS** Radar signal recognition, Cohen class time-frequency distribution, convolutional neural network, deep Q-learning network.

## I. INTRODUCTION

Intra-pulse modulation recognition of radar signals is an important part of modern electronic intelligence reconnaissance and electronic support systems [1], [2]. Correct recognition of intra-pulse modulation of radar signal can not only help to deduce the function of enemy radar, thus judging its threat level, but also improve the accuracy of parameter estimation. Due to the increasing density of radar signals in the modern electronic warfare environment and the use of large time-width pulse compression signals with complex modulation in most modern radar signals [3], [4], radar

reconnaissance systems often intercept overlapping pulses in time and frequency domains to form the multi-component radar emitter signals [5]. Most of the proposed modulation recognition technologies are not adaptable to the multi-component signal environment, resulting in failures in modulation recognition. Therefore, the analysis and processing of multi-component signals is an urgent problem in the current radar reconnaissance system.

The research of intra-pulse modulation recognition of radar signal is mainly focused on the single-component signal. Radar signal intra-pulse modulation recognition methods for single-component signal can be divided into the following two categories: traditional feature extraction methods [6]–[8] and the methods based on deep learning [9]–[12].

The associate editor coordinating the review of this manuscript and approving it for publication was Naveed Akhtar<sup>ID</sup>.

Traditional recognition methods of feature extraction can be divided into two parts: feature extraction and classification. For feature extraction, scholars have proposed feature extraction methods based on fractional Fourier transform [6], [8], short-time Ramanujan Fourier transform [7], integrated quadratic phase function [8] and other feature extraction methods. However, the generalization performance and anti-noise performance of these methods are poor, and it is difficult to meet the needs of current radar intra-pulse modulation recognition. In recent years, due to the optimal features can be automatically extracted based on deep learning, the recognition method of deep learning has been applied in the field of radar signal intra-pulse modulation recognition. In [9], a CNN is explored to identify radar signals based on radar signals' Choi-Williams distribution (CWD). The method can recognize 8 kinds of radar signals when the SNR is above  $-2$  dB. In [10], CNN and deep encoder are used to recognize TFIs of radar signals. The method can recognize 12 kinds of radar signals. The overall PSR is 95.5% when the SNR is  $-6$  dB. The recognition method based on deep learning can effectively improve the overall PSR at low SNR and adapt to the recognition of a wide range of radar signal types.

In previous studies, the research on multi-component signal mainly focused on multi-component signal separation [5], [13]–[16]. Scholars have proposed multi-component signal separation methods based on parameterized time-frequency analysis [5], [13], time-frequency image processing [14] and blind source separation [15], [16]. Recently, some researchers have proposed radar signal intra-pulse modulation recognition methods based on multi-component signal separation [17], [18]. Reference [17] decompose received signals into multiple components based on fractional Fourier transform and then identifies each signal component separately based on CNN and fusion features. The method can separate and recognize 9 kinds of overlapping radar signals. The overall PSR of dual-component signals is 72% when the SNR is 0 dB. In [18], regression variational mode decomposition is explored to separate the received signals, and then identifies the first signal component and second signal component based on deep belief network (DBN) and fusion network, respectively. The method can separate and recognize 8 kinds of overlapping radar signals. The overall PSR of dual-component signals is 94% when the SNR is 0 dB. However, there are still many problems in the method of intra-pulse modulation recognition for multi-component radar signals. First, signal separation algorithms usually need a lot of iteration and search processes, and the amount of computation is large. Second, the recognition effect of recognition methods largely depends on the separation effect of signal separation algorithms, but the separation ability of the proposed separation methods in the low SNR environment is poor, which limits the recognition ability of the methods. Finally, the proposed methods assume that the number of signals contained in the current signal is known, and design the recognition methods for single-component signals and

dual-component signals, respectively, which is difficult to meet the problem of radar intra-pulse modulation recognition with unknown number of the signals.

In this paper, we propose a novel approach for single-component and dual-component radar signal intra-pulse modulation recognition based on the network architectures for multi-label image classification [19]–[21]. The approach can identify 8 kinds of random overlapping typical radar signals, including linear frequency modulation (LFM), mono-pulse (MP), sinusoidal frequency modulation (SFM), binary phase-shift keying (BPSK), binary frequency shift keying (2FSK), quaternary frequency shift keying (4FSK), even quadratic frequency modulation (EQFM) and Frank code. First, we extract the TFIs of received signals by CTFD with multiple kernel functions. Besides, we adopt image processing techniques to suppress noise and adjust the size and magnitude of the TFIs. Second, we design and pre-train a TFI feature extraction network for radar signals based on CNN. Finally, to improve the PSR of the recognition system in the pulse overlapping environment, a multi-label classification network based on a DQN is explored. Besides, two sub-networks take TFIs based on special kernel functions as input and re-judge the recognition results of some specific signals to further enhance the recognition effect of the recognition system. The simulation results show that the overall PSR of dual-component radar signals can reach 94.83% when the SNR is  $-6$  dB. The approach is also adaptable to the recognition of intra-pulse modulation of single-component radar signals.

This paper is organized as follows: Section II introduces the recognition system structure and the radar signal model. And we introduce the signal preprocessing in Section III. Feature extraction network and multi-label classification network are introduced in Section IV and section V, respectively. Section VI shows the simulation results. Finally, Section VII provides conclusions.

## II. SYSTEM STRUCTURE AND SIGNAL MODEL

### A. SYSTEM STRUCTURE

In this paper, we propose a novel radar signal intra-pulse modulation recognition approach. The whole recognition system consists of three parts, including signal preprocessing, TFI feature extraction and multi-label classification for radar signals. The system structure of the proposed approach is shown in Fig. 1.

First, the received radar signals are preprocessed. We extract the TFIs of received signals by CTFD with multiple kernel functions. The first kernel function has a relatively wide range of radar signal adaptability, which is used as input of the main network of the recognition system. The second and third kernel functions have a better time-frequency analysis effect than the first kernel function for some specific signals and are used to adjust the recognition results of the main network. Besides, the image processing methods are used to suppress noise and adjust the size and amplitude of the TFIs. Second, in view of the strong feature

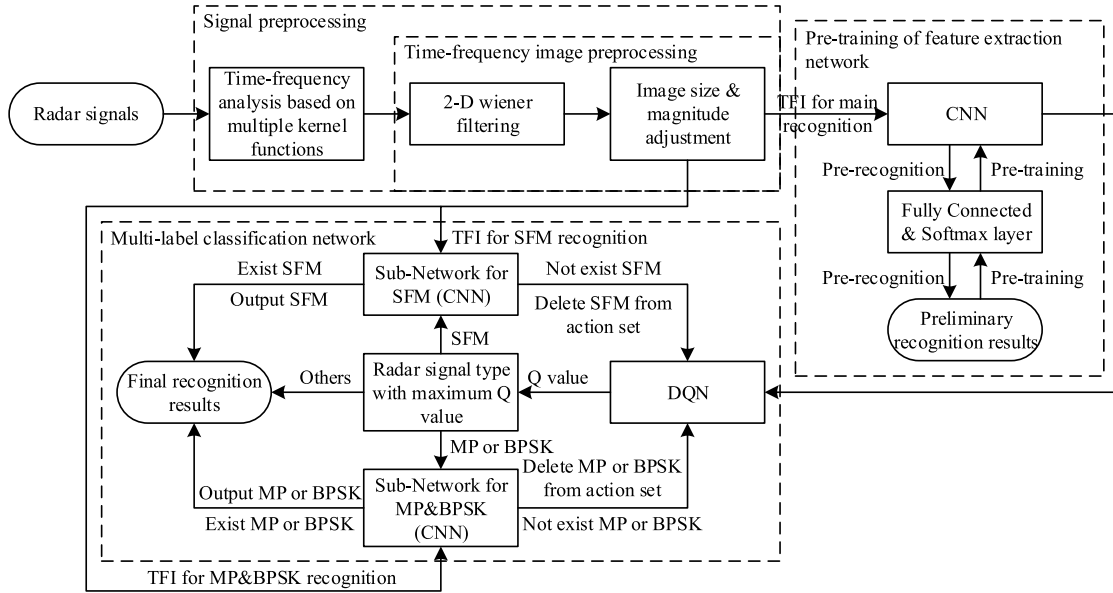


FIGURE 1. Radar signal intra-pulse recognition system structure.

extraction ability of CNN, we combine the CNN, the fully connected layer and the Softmax layer to extract TFI features of the radar signals. After pre-training the TFI feature extraction network, the parameters of CNN are preserved. Finally, to improve the PSR of the recognition system in the pulse overlapping environment, a multi-label classification network based on a DQN is explored. Besides, aiming at the SFM signal with poor recognition effect in the main network and the easily confused MP and BPSK signal, two sub-networks are designed based on CNN. The TFIs generated by special kernel functions are used as input to re-judge the recognition results of SFM, MP and BPSK signals to further enhance the PSR of the recognition system.

**B. RADAR SIGNAL MODEL**

The signal intercepted by the passive radar system includes modulated radar signal and channel noise. The intercepted signal model can be expressed as follows:

$$\begin{aligned}
 x(t) &= \sum_{i=1}^k s_i(t) + n(t) \\
 &= \sum_{i=1}^k A_i \text{rect}(t/T_i) e^{j(2\pi f_c t + \phi_i(t) + \phi_{0_i})} + n(t) \quad (1)
 \end{aligned}$$

where,  $s_i(t)$  and  $n(t)$  represent the  $i$ th signal component of the modulated radar signal and channel noise, respectively. The channel noise is generally assumed to be additive white Gaussian noise.  $k$  is the number of signal components of the modulated radar signal.  $A_i, T_i, f_{c_i}$  and  $\phi_{0_i}$  represent the amplitude, the pulse width, the carrier frequency and the initial phase of the  $i$ th signal component, respectively.  $\phi_i(t)$  represent phase function of the  $i$ th signal component, which is the main difference of intra-pulse modulations of radar signals.

In the problem of multi-component radar signal recognition, there is little difference in energy between overlapping signals which interact with each other. So we assume that the overlapped signals have the same amplitudes, and we set  $A_i = 1$ . In the follow-up study of this paper, we only consider the situation with a large probability in the actual battlefield, that is, the signal intercepted by the radar system is a single-component signal or dual-component signal, where the dual-component signal is formed by overlapping two signals. So we set  $1 \leq k \leq 2$ .

**III. SIGNAL PREPROCESSING**

In this section, we introduce the time-frequency analysis method and the TFI preprocessing methods, including CTFD, two-dimensional Wiener filtering, image size adjustment and image amplitude normalization, so as to facilitate the data processing of subsequent neural networks.

**A. TIME-FREQUENCY ANALYSIS**

CTFD is a bilinear time-frequency distribution, which is expressed as follows [12]:

$$P(t, \omega; \phi) = \frac{1}{4\pi^2} \iiint x(u + \frac{\tau}{2}) x^*(u - \frac{\tau}{2}) \phi(\tau, \nu) e^{-j(\nu t + \tau \omega - \nu u)} du d\tau d\nu \quad (2)$$

where  $t$  and  $\omega$  are time axis and frequency axis in the time-frequency domain.  $x(t)$  is the intercepted signal.  $\phi(\tau, \nu)$  is a kernel function for filtering in the ambiguity domain.  $\tau$  and  $\nu$  are the time-delay axis and frequency-shift axis in the ambiguity domain, respectively.

The self-term energy of the signal in the ambiguity domain is mainly concentrated near the origin, so the kernel function is designed as a low-pass filter in the ambiguity domain.

CTFD based on different kernels has different time-frequency analysis characteristics. Reference [12] proposed a kernel function base on the characteristics of radar signals, and the expression of the kernel function is as follows:

$$\phi_1(\tau, \nu) = e^{-(\alpha\tau^2 + \beta\nu^2)} \quad (3)$$

where  $\alpha$  and  $\beta$  are used to adjust the shape and size of the kernel function. The simulation result of [12] shows that the CTFD based on this kernel function has better time-frequency analysis ability than CWD. In this paper, we adopt the CTFD proposed in [12] to obtain TFIs with good quality, and we set  $\alpha = 0.0005$ ,  $\beta = 0.001$ . In subsequent processing, the obtained TFIs are preprocessed and inputted into the main recognition network. Fig.2 is the TFIs of 8 typical radar signals without overlap obtained by CTFD.

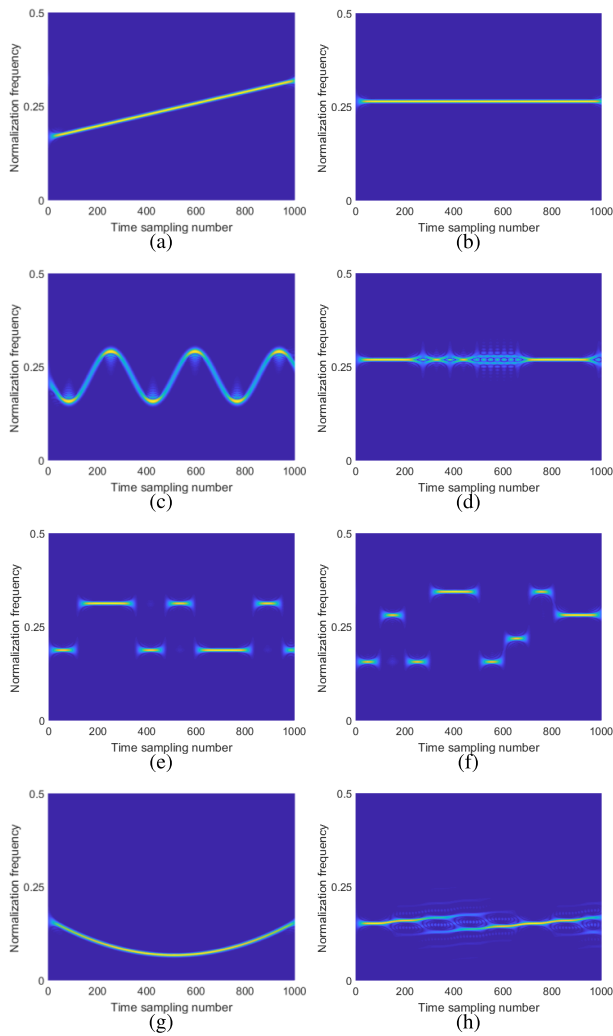


**FIGURE 2.** The TFIs of 8 typical radar signals without overlap obtained by CTFD: (a) LFM, (b) MP, (c) SFM, (d) BPSK, (e) 2FSK, (f) 4FSK, (g) EQFM, (h) Frank code.

The kernel function proposed in [12] is suitable for a wide range of radar signal types. However, it is difficult for a single kernel function to fully adapt to all radar signal types.

Therefore, we design new kernel functions and adjust the parameters of the kernel functions for several radar signals that perform poorly in the above-mentioned TFIs, and acquire additional TFIs that are specific to some radar signals.

The SFM radar signal studied in this paper has a high frequency modulation (FM) slope. The kernels proposed in [12] filter out the energy of the signal with a high FM slope, which results in a poor time-frequency aggregation in the TFI. Therefore, according to the signal energy distribution characteristics of SFM in the ambiguity domain, a new butterfly kernel function is proposed. The expression of the kernel function is as follows:

$$\phi_2(\tau, \nu) = e^{-(\gamma\tau^2 + \varepsilon(\nu/\tau)^2)} \quad (4)$$

where  $\gamma$  and  $\varepsilon$  are used to adjust the shape and size of the kernel function. In this paper, we set  $\gamma = 0.0005$ ,  $\varepsilon = 0.025$ . The contour map of the new kernel function presented in this paper is shown in Fig.3. The TFI obtained by CTFD based on the kernels proposed in [12] and the new kernels proposed in this paper is shown in Fig.4. It can be seen that the TFI obtained by CTFD based on the new kernel function presented in this paper has higher time-frequency aggregation. In subsequent processing, the CTFD based on the new kernel function is preprocessed and inputted into the SFM radar signal recognition sub-network to improve the recognition accuracy of the SFM radar signal.

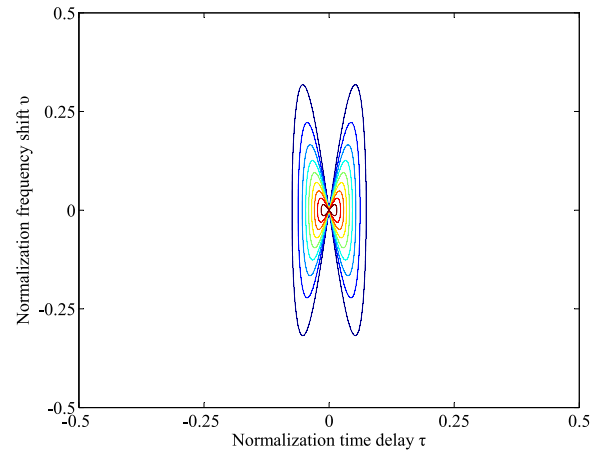


**FIGURE 3.** The contour map of the new kernel function designed by this paper.

In addition, TFIs under low SNR are seriously affected by noise. The curves of MP radar signals in TFIs may break, which are similar to the TFI characteristics of BPSK radar signals, resulting in confusion between recognition of MP radar signals and BPSK radar signals. In the ambiguity domain, the main energy of MP radar signals and BPSK radar signals is distributed on the time-delay axis. Therefore, the TFI quality of MP radar signals and BPSK radar signals can be improved by adjusting the parameters of the kernel function in [12] and extending the width of the low-pass filter window of the kernel function in the direction of the time-delay axis. In this paper, we set  $\alpha = 0.0001$ ,  $\beta = 0.001$ .



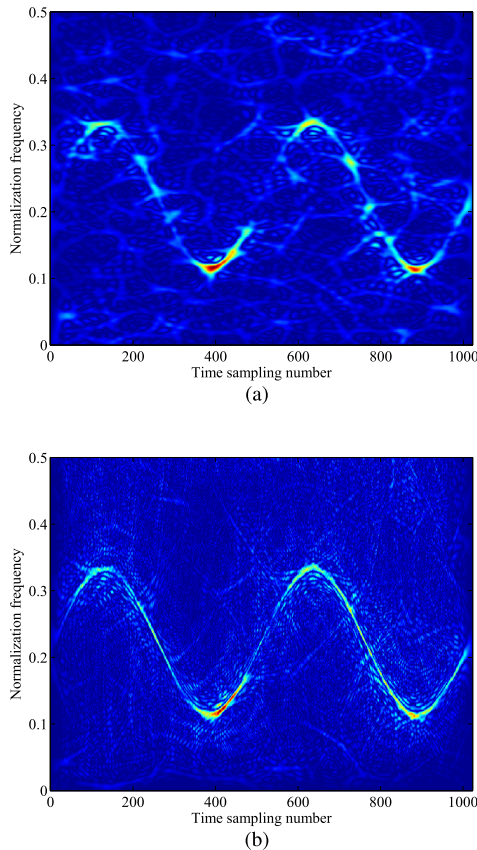


**FIGURE 4.** The TFIs of the SFM signal obtained by CTFD when SNR is  $-6$  dB: (a) CTFD based on the kernel function proposed in [12], (b) CTFD based on the new kernel function proposed in this paper.

In subsequent processing, the obtained TFIs are preprocessed and inputted into the MP and BPSK radar signal recognition sub-network to improve the recognition effect of MP and BPSK radar signals.

**B. TIME-FREQUENCY IMAGE PREPROCESSING**

In order to facilitate the data processing of subsequent deep networks, this paper adopts similar image processing methods of [12] to preprocess the TFIs. First, we use two-dimensional Wiener filtering to suppress the noise of the TFIs. Then we use bilinear interpolation to adjust the size of

the TFIs. The difference is that the size of the adjusted image is different. The TFIs with  $64 \times 64$  size are easy to lose details in the multi-component signal environment, so we adjust the size of the TFIs to  $96 \times 96$ . Finally, since the signals interfere with each other in the multi-component signal environment, the signal data may be lost during the binarization process. Therefore, we use the amplitude data of the TFIs as the input of the deep network. In addition, in order to standardize the data input of the deep network, we normalize the amplitude of the TFIs. The normalization method adopted in this paper is maximum normalization, which divides the amplitude of each pixel of the TFI by the maximum amplitude to get the normalized TFI output.

**IV. PRE-TRAINING OF FEATURE EXTRACTION NETWORK**

This section mainly introduces the details of the TFI feature extraction network in this paper. The output structure of CNN is modified according to the label form of the radar signals, and the CNN is pre-trained. The purpose of this step is to get the TFI feature extractor based on CNN.

In view of the powerful image feature extraction capability of CNN, most of the recent radar signal recognition methods used CNN as a TFI feature extractor [9]–[12]. The basic CNN structures only consider the single-label classification task [22], [23]. In order to deal with the recognition task of the intra-pulse modulation type of the single-component and dual-component radar signals, we expand the output part of CNN according to the signal label form of the radar signals.

The radar signal pulse studied in this paper contains at most two signal components. The form of the signal label is as follows:

$$l = (m_1, m_2), \quad m_1 \in \{1, 2, \dots, 8\}, \quad m_2 \in \{1, 2, \dots, 9\} \quad (5)$$

The label values 1 to 8 correspond to the 8 types of intra-pulse modulation of radar signals studied in this paper. For single-component signals, the first label is the modulation type of the signal, and the second label is “empty”, which is expressed by the label value 9. Based on the signal label form in this paper, the structure of CNN after extending the output part is shown in Fig.5.

This paper designs a network structure based on the input data form of the CNN. First, the form of the TFIs as the input

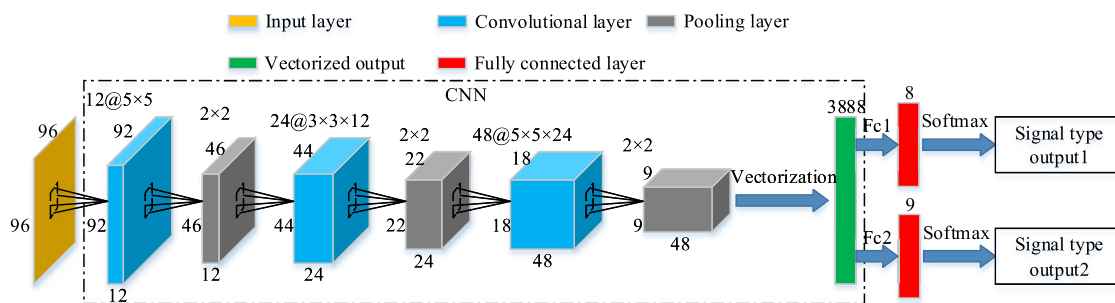


**FIGURE 5.** The structure of CNN after extending the output part.

data of the CNN is simple. Therefore, the convolution part of the CNN designed in this paper contains only 3 convolutional layers and 3 pooling layers. Secondly, the size of the convolutional kernel is designed according to the width of the time-frequency curves in the TFIs. In the TFIs, the width of the time-frequency curves of the radar signals is about 2 to 3 pixels. In order to capture the subtle characteristics and changes of the time-frequency curve trend, this paper designs the convolutional kernel size of the CNN as  $5 \times 5$ . Finally, in the second layer, if the convolutional kernel with the size of  $5 \times 5$  is used, the feature map size of the output through the calculation of the second layer is  $21 \times 21$ , which leads to the need for padding operation in the pooling layer of the third layer. For the average pooling adopted in this paper, noise interference may be caused by edge padding operation. Therefore, in order to avoid padding operation, the size of the convolutional kernel of the second layer is adjusted to  $3 \times 3$ . After the convolution and pooling calculations, the feature maps output by the last pooling layer are vectorized into feature vectors. Then the recognition results of two signal components are corresponded by two fully connected layers, respectively, and the recognition results are transformed into probability values through the Softmax layer. It is worth noting that the output structure of the recognition results of the two signal components is slightly different. To deal with the recognition problem of single-component signals, the output of the second signal component contains 9 neurons, and the output of the second signal component contains an additional neuron corresponding to the signal type of "empty". After the output of the network is obtained through the Softmax layer, the error between the output vector and the label vector is calculated, and the parameters of the feature extraction network are adjusted by the back propagation algorithm.

After pre-training the feature extraction network, the parameters of CNN in the feature extraction network are reserved. In the subsequent processing, the features of the TFIs are extracted by CNN, and the recognition results are output by the multi-label classification network.

### V. MULTI-LABEL CLASSIFICATION NETWORK

In this section, the fully connected layer and the Softmax layer of the neural network in the previous section are replaced by a recurrent neural network (RNN). The classification results are output through multiple cyclic iterations. Then the designed RNN is used as the network structure of DQN and trained by the deep Q-learning algorithm. Finally, two sub-networks are designed to adjust the recognition results of DQN to obtain higher PSR.

#### A. DESIGN OF RECURRENT NEURAL NETWORK

Standard CNN uses the fully connected layers and Softmax layers to establish the mapping relationship between feature vectors and signal modulation types. In the previous section, the mapping relationship between feature vectors and multiple signal component modulation types is established by combining multiple fully connected layers with Softmax

layers. However, the classification of each signal is based on the same feature vector, which is not conducive to multi-label classification. Besides, the relationship between the classification results of modulation types of each signal component is not established, so its recognition ability is limited. In the field of deep learning, reference [19] proposed a method combining CNN and RNN to solve the problem of multi-label image recognition, and achieves good recognition results. In this paper, the classification network is designed based on the RNN structure to establish the relationship between the multi-component radar signal classification process. The current classification process can refer to the classification results of the previous steps, so as to improve the accuracy of the classification network. The RNN structure is shown in Fig.6.

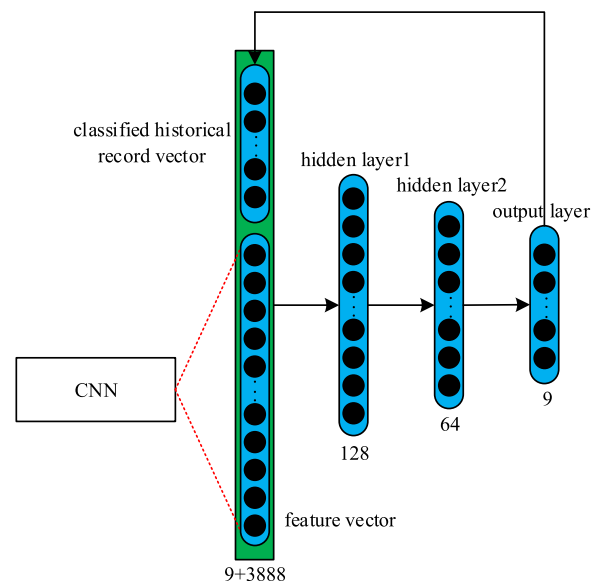


FIGURE 6. The RNN structure designed for classification in this paper.

The inputs of RNN are composed of two parts: the feature vectors of TFIs and the classified historical record vectors of RNN. The input vector can be expressed as follows:

$$I = (f, ch) \tag{6}$$

where  $I$  is the input vector of RNN,  $f$  is the feature vector of TFI, and  $ch$  is the classified historical record vector of RNN.

The interconnect structure of the recurrent neural network is fully connected. Two hidden layers use rectified linear unit (ReLU) as the activation function. In order to facilitate the subsequent DQN to calculate the Q value, the output layer does not use the activation function. The calculation process of each layer is as follows:

$$\begin{aligned} h_i &= \text{ReLU}(z_i) = \text{ReLU}(W_i x_i + b_i) \\ &= \max(0, W_i x_i + b_i), \quad i \in \{1, 2\} \end{aligned} \tag{7}$$

$$o = W_o h_2 + b_o \tag{8}$$

where  $h_i$  and  $o$  are the output values of the  $i$ th hidden layer and the output layer, respectively.  $x_i$  is the input of the

$i$ th hidden layer.  $\theta_i = (W_i, b_i)$  is the parameter of the  $i$ th hidden layer, and  $\theta_o = (W_o, b_o)$  is the parameter of the output layer.

Based on the feature vectors extracted by CNN in the previous section, the RNN outputs the recognition results of intra-pulse modulation types of single-component and dual-component radar signals through multiple cyclic iteration classification processes.

### B. DESIGN OF DEEP Q-LEARNING NETWORK

In order to improve the accuracy of the classification network, this paper adopts the reinforcement learning to train the RNN designed in the previous step. The traditional training label of supervised learning usually adopts the form of one-hot code, which strictly limits the output value of the deep network model. In this paper, a training mode based on reinforcement learning is introduced. According to the label set of the single-component and dual-component radar signals, a reward value is fed back to the classification network, and the parameters of the network are updated by the reward value. Based on the above reward and punishment rules in reinforcement learning, the classification network can choose the order of output of recognition results autonomously to avoid the hard restriction of traditional classification network labels and improve the adaptability of classification network to the recognition of complex dual-component radar signals formed by pulse overlapping. Reinforcement learning agents can achieve the optimal strategy through interaction with the environment and continuous trial-and-error learning [24]. Reinforcement learning has three elements, the first one is state, the second one is action, and the third one is reward. The basic process of reinforcement learning is as follows: at time  $t$ , the state of the agent is  $s_t$ . By observing the environment, taking action  $a_t$ , and getting feedback  $r_t$  from the environment, the agent enters the next state  $s_{t+1}$  and repeats the process until the interaction ends. For the recognition of intra-pulse modulation of radar signals in this paper, the RNN obtained in the previous step can be regarded as an agent of reinforcement learning. In this part, we train the agent with the deep Q-learning algorithm and get the agent with multi-label classification ability, which is DQN. The training and recognition process of DQN is shown in Fig.7.

The state vector of DQN is the input vector of RNN in the previous part. The state vector changes with the classification result of the network output before the current step. Then DQN classifies according to the current state.

The action taken by DQN is to select a signal modulation type in a recurrent step, which corresponds to the recognition result of a signal component in the current signal. DQN obtains recognition results through two classification processes. The recognition results are in the same form as the signal labels mentioned in the previous section, and the action space  $A$  corresponds to the label set, that is, the action space in this paper contains 9 kinds of actions.

The feedback of the environment is obtained by comparing the recognition results with the signal labels.

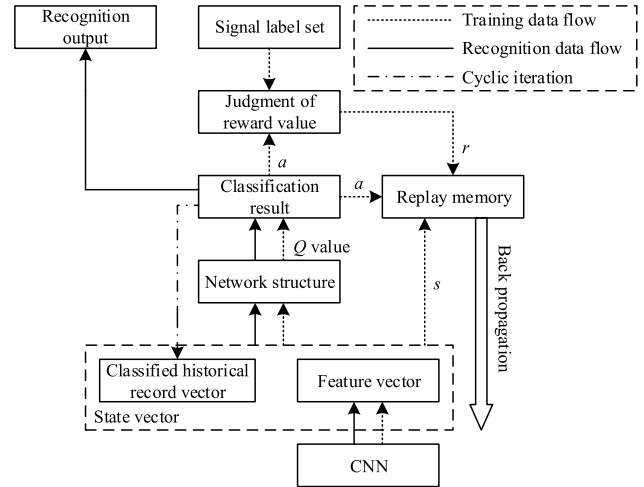


FIGURE 7. The training and recognition process of DQN.

The environment feedback space  $R$  includes two values of  $-1$  and  $1$ , which reflect the quality of network output. If the recognition result belongs to the current radar signal label set, the environment feedback gives the network a positive value, and the identified label is removed from the radar signal label set, otherwise, the environment feedback gives the network a negative value.

The training process can be described by Algorithm 1, where the input is the feature vectors of TFIs, the output is

#### Algorithm 1 Deep Q-Learning Network Training Process

**Require:**  $f$   
**Ensure:**  $\theta = (\theta_1, \theta_2, \theta_o) = ((W_1, b_1), (W_2, b_2), (W_o, b_o))$

- 1: Initialize  $\theta, D$ ;
- 2: **for** each TFI **do**
- 3:   Initialize  $ch$
- 4:   **for** each  $step = 1 : 2$  **do**
- 5:      $o \leftarrow Q_\theta(s_{step}) \leftarrow Q_\theta(f, ch)$
- 6:     Select action  $a_{step}$  based on  $o$  and  $\epsilon$ -greedy policy;
- 7:     Execute action  $a_{step}$  and observe reward  $r_{step}$ ;
- 8:     Update  $ch$  and get the flag of termination status  $ts_{step}$ ;
- 9:   **end for**
- 10:   **for** each  $step = 1 : 2$  **do**
- 11:     Store  $(s_{step}, a_{step}, r_{step}, s_{step+1}, a_{step+1}, ts_{step})$  in  $D$ ;
- 12:   **end for**
- 13:   Random sampling  $m$  samples from  $D$  to calculate  $Q_{target}$ ;  
    Samples:  
     $(s_j, a_j, r_j, s_{j+1}, a_{j+1}, ts_j), j \in \{1, 2, \dots, m\}$ ;
- 14:    $Q_{target}^{(j)} \leftarrow \begin{cases} r_j & ts_j \text{ is true} \\ r_j + \gamma \max(Q_\theta(s_{j+1}, a_{j+1})) & ts_j \text{ is false} \end{cases}$
- 15:    $L \leftarrow \frac{1}{2m} \sum_{j=1}^m (Q_{target}^{(j)} - Q_\theta(s_j, a_j))^2$ ;
- 16:    $\frac{\partial L}{\partial \theta} \leftarrow$  Back propagation;
- 17:    $\theta \leftarrow \theta - \alpha \frac{\partial L}{\partial \theta}$ ;
- 17: **end for**

all the parameters of the network, including the parameters of two hidden layers and the parameters of the output layer,  $D$  is replay memory,  $\varepsilon$  is exploration rate,  $\gamma$  is attenuation factor, and  $\alpha$  is learning rate.

The network parameters are obtained through the training process. The Q value of each action is calculated forward by using the feature vector of the TFI extracted by CNN. The action with the highest Q value is adopted to obtain the recognition result of the first signal component. Then the state vector is updated and entered the next cycle. After the same operation, the recognition result of the second signal component is obtained. Besides, to further improve the recognition effect of the recognition system, we use sub-network to adjust the recognition result of DQN in the next part.

### C. DESIGN OF SUB-NETWORK BASED ON CNN ARCHITECTURE

In the time-frequency analysis procession of Section III, we obtain two additional TFIs according to the energy distribution characteristics of SFM, MP and BPSK radar signals in the ambiguous domain besides the TFIs of the main recognition network. In this part, two additional TFIs obtained in Section III are processed based on CNN architecture. The two recognition sub-networks designed in this paper have the same convolution structure as the feature extraction network in Section IV. The difference is the fully connected layer and the Softmax layer of the output part.

If the recognition result of a certain radar signal component output by the DQN is SFM radar signal, the SFM radar signal recognition sub-network is enabled. TFI based on the second kernel function is used as the input of SFM radar signal recognition sub-network. The output of the sub-network contains 2 neurons, which respectively represent the probability of including and not including SFM radar signal components in the current radar signal pulse. If the recognition result of the sub-network is that the current pulse contains the SFM radar signal component, the SFM radar signal is directly output as the final recognition result. If the recognition result of the sub-network is that the current pulse does not contain the SFM radar signal component, the SFM radar signal will be deleted from the action set, and the recognition result will be reselected according to the Q value output by the DQN.

The process of MP and BPSK radar signal recognition sub-network is similar to that of SFM radar signal recognition sub-network. The sub-network is enabled when the recognition result output by the DQN is MP or BPSK radar signal. The output of the sub-network consists of 4 neurons, which represent the probability that MP and BPSK radar signal components are included or not in the current radar signal pulse. When the recognition result of the sub-network is that the current pulse contains MP or BPSK radar signal component, the recognition result of the DQN will be output directly as the final recognition result, otherwise, the MP or BPSK radar signal will be deleted from the action set, and the recognition result will be reselected according to the Q value output by the DQN.

Finally, when the recognition result of the DQN is other radar signal types except for MP, BPSK, and SFM, the recognition result of the DQN is directly output as the final recognition result. According to the above process, this paper adjusts the recognition result of the DQN by combining with the sub-networks, obtains the final recognition result and completes the recognition.

## VI. SIMULATION RESULT AND DISCUSSION

In this section, the recognition performance of the proposed method under different SNRs is analyzed by simulation. The SNR is defined as  $SNR = 10\log_{10}(\sigma_s^2/\sigma_n^2)$ ,  $\sigma_s^2$  and  $\sigma_n^2$  are signal power and noise power, respectively. There are 8 kinds of simulated radar modulation signals. The types and parameters are shown in Table 1. The sampling points of each signal are between 1024 and 2048. The SNR of training set samples ranges from  $-6$  dB to  $10$  dB. Every  $2$  dB,  $4000$  single-component or random overlapping dual-component signal samples satisfying Table 1 are generated. Among them, the sample ratio of single-component signal and overlapping dual-component signal is  $1:4$ , and  $36000$  samples are generated as the training set. The SNR of the test set samples ranges from  $-10$  dB to  $10$  dB. In the same way as the training set,  $44000$  single-component signal samples and  $44000$  overlapping dual-component signal samples are generated, respectively. A total of  $88000$  samples are generated as the test set.

TABLE 1. Simulation radar signal parameter table.

Signal type	Parameter	Range
LFM	Initial frequency ( $f_i$ )	$0.1 - 0.4$
	Bandwidth( $\Delta f$ )	$0.1 - 0.3$
MP	Carrier frequency ( $f_c$ )	$0.1 - 0.4$
SFM	Minimum frequency ( $f_{min}$ )	$0.1 - 0.2$
	$\Delta f$	$0.1 - 0.3$
BPSK	Barker codes	$[7,11,13]$
	$f_c$	$0.1 - 0.4$
	Symbol width ( $T_s$ )	$(1/20 - 1/15) * N$
2FSK	$f_{c1}, f_{c2}$	$0.1 - 0.4$
4FSK	$T_s$	$(1/32 - 1/8) * N$
	$f_{c1} - f_{c4}$	$0.1 - 0.4$
EQFM	$T_s$	$(1/32 - 1/8) * N$
	$f_{min}$	$0.1 - 0.4$
Frank	$\Delta f$	$0.1 - 0.3$
	$f_0$	$0.1 - 0.4$
	$T_s$	$(1/100 - 1/32) * N$
	Phase number ( $M$ )	$[4,5,6,7]$

The frequency value in the table is the normalized frequency based on the sampling frequency  $f_s$ . According to Nyquist sampling law, the sampling frequency should be more than or equal to 2 times of signal carrier frequency, and the range of normalized carrier frequency is  $(0,0.5]$ . The symbol width and signal length in this paper are expressed by sampling points  $N$ . The time length corresponding to the sampling points is related to the sampling frequency of the receiver. The corresponding time length of  $N$  sampling points is  $N/f_s$ .

### A. THE EFFECT OF CLASSIFICATION NETWORK BASED ON DQN

In order to evaluate the recognition effect of the recognition system, this paper defines the following criteria: if the recognition result is identical with the modulation mode



of the signal components contained in the current single-component or dual-component signal, the current recognition result is correct, otherwise, the current recognition result is wrong. Based on the above rules, the probability of successful recognition of the proposed recognition system is obtained by the simulation tests, which is called the overall PSR.

For the multi-label classification network structure, we use CNN as a feature extractor. Based on the extracted feature vectors, we simulate the overall PSR of the traditional fully connected layer classification network and the DQN-based classification network, respectively. As can be seen from Fig.8, in the low SNR environment, the classification network based on DQN can obtain a higher overall PSR. When the SNR is  $-6$  dB, the classification network based on DQN can increase the overall PSR from 82.95% to 94.03%. And when the SNR is  $-8$  dB, the classification network based on DQN can increase the overall PSR from 57.13% to 74.75%. The simulation results show that the classification network based on DQN has a more accurate multi-classification decision ability for dual-component radar signal recognition. This is mainly because the DQN network obtains classification results through multiple classification decisions, and in each classification process, it refers to the classification results of the previous cycle steps, establishes the relationship between the classification results, and makes more accurate classification decisions.

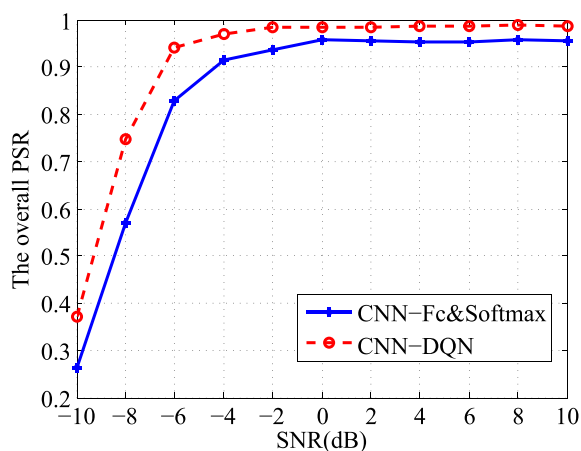


FIGURE 8. The effect of DQN on the overall PSR of the proposed approach.

**B. THE EFFECT OF SUB-NETWORK PROCESSING AND RECOGNITION EFFECT OF DUAL-COMPONENT RADAR SIGNALS**

For dual-component signals, the recognition results include multiple radar signal types. The PSR defined for single-component signals is not enough to describe the recognition effect of each signal type. In this paper, two indexes in the field of deep learning are introduced to describe the classification effect of the approach, including precision rate and recall rate.

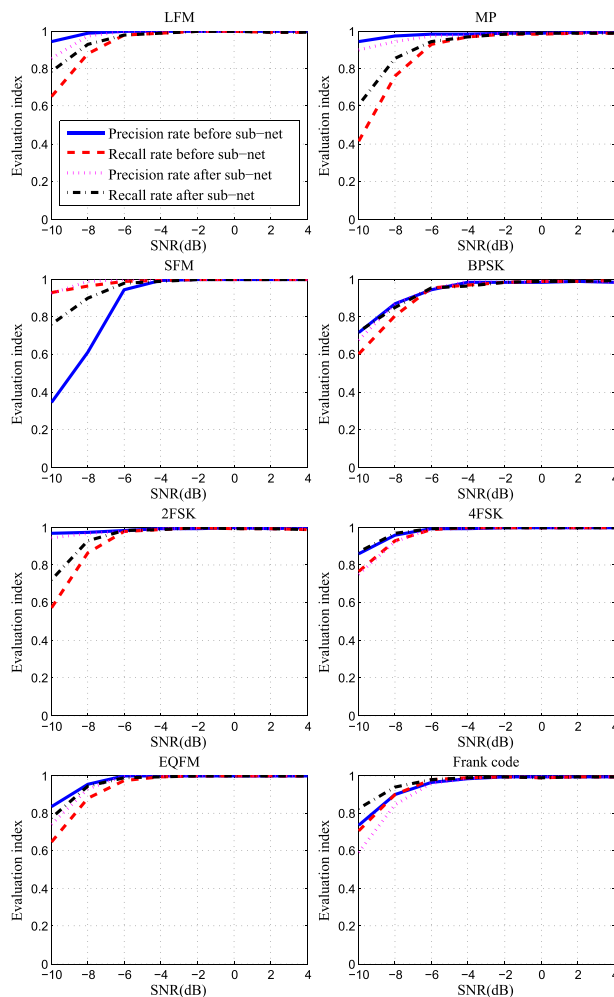


FIGURE 9. The precision rate and recall rate of 8 kinds of radar signals before and after sub-network processing in dual-component signal environment.

Fig.9 shows the precision rate and recall rate of 8 radar signals before and after sub-network processing in the dual-component signal environment. It can be seen from the figure that the problem of the recognition results before sub-network processing mainly focuses on MP and SFM signals: at low SNR, the precision rate of SFM signals is low, while the recall rate of MP signals is low. SFM signals have poor time-frequency clustering, which can cause a large number of false recognition at low SNR, and it also leads to low recall rate of radar signals of other modulation types; MP signals and BPSK signals are confused at low SNR, which is manifested by the missing recognition of MP signals and the false recognition of BPSK signals. By comparing the precision rate and recall rate of the signal before and after sub-network processing, it can be seen that the precision rate of SFM radar signal has been greatly improved at low SNR, and the recall rate of MP radar signal is also significantly improved. In the processing of the two subnetworks, the accuracy of the BPSK radar signal will be improved and reduced respectively. Under the joint action of the two sub-networks, the recognition effect of the BPSK radar signal has hardly changed.



In addition, the recall rate of other modulated radar signals has been improved to varying degrees, while the precision rate is slightly reduced. The overall recognition effect of the recognition system is better than that before sub-network processing. From Fig.10, it can be seen that after the sub-network processing, the overall PSR of the recognition system in the low SNR environment is significantly improved. The sub-network can increase the overall PSR from 74.75% to 83.05% when the SNR is  $-8$  dB. This is mainly because the TFIs as the input of the sub-networks have high pertinence to the specific signals. The recognition results of the sub-networks for the specific signals have high accuracy.

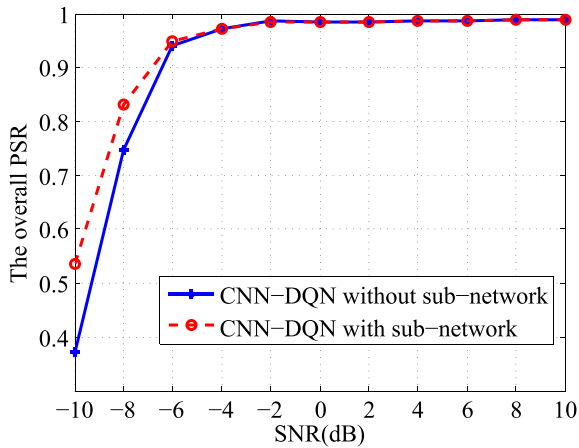


FIGURE 10. The effect of sub-network on the overall PSR of the proposed approach.

Fig.9 shows the precision rate and recall rate of 8 radar signals after sub-network processing, and Fig.10 shows the overall PSR after sub-network processing, that is, the recognition effect of the dual-component radar signal of the whole recognition system. It can be seen from the figure that the precision rate and recall rate of all signal types are above 90% and the overall PSR is 94.83% when the SNR is  $-6$  dB. When the SNR is  $-8$  dB, the precision rate and recall rate of all radar signal types are still above 85%. This shows that the approach has good recognition performance for dual-component radar signals at low SNR.

### C. RECOGNITION EFFECT OF SINGLE-COMPONENT RADAR SIGNALS

The recognition system should have adaptability for the recognition of single-component radar signals which are more common in the actual battlefield. Fig.11 shows the PSR of 8 kinds of radar signals studied in this paper and the overall PSR. When the SNR is  $-6$  dB, the PSR of all signal types are above 85%, and the overall PSR is 94.43%. From the recognition results of single-component radar signal, it can be seen that the PSR of single-component radar signal is slightly lower than that of dual-component radar signal, because the recognition system in this paper adopts the same recognition process for single-component radar signal and dual-component radar signal, and there is no essential

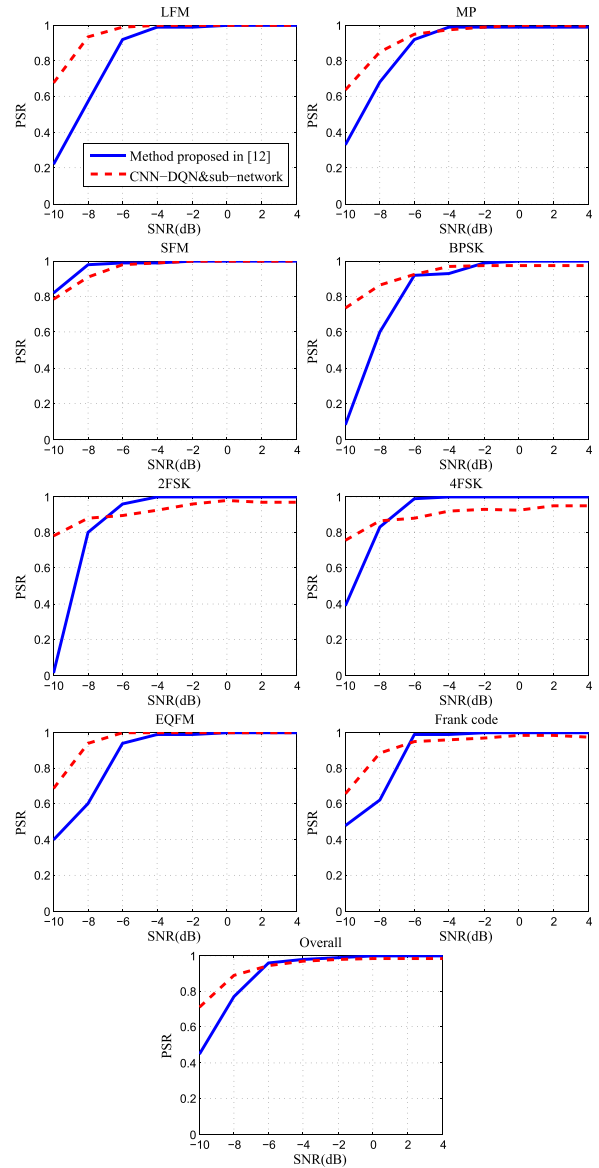


FIGURE 11. The PSR of 8 kinds of single-component radar signals and the overall PSR.

difference for the recognition process in both cases. For the recognition of the single-component radar signal, only when the two labels given by the recognition system are the correct recognition result of single-component radar signal and “empty”, can we think that the recognition result of the recognition system is correct. The error of single-component radar signal recognition in simulation analysis is mostly due to the recognition of single-component radar signals into the same modulated dual-component radar signals in this paper, especially for the recognition of FSK radar signals.

To further verify the recognition effect of this approach for single-component radar signals, we compare the approach of this paper with the existing approach (based on [12]). It can be seen from Fig.11, the approach proposed in this paper and the approach in [12] have their advantages for single-component signal recognition. The approach presented in this paper has a better recognition effect for LFM, MP, BPSK and EQFM

signals than the method in [12], especially in low SNR environment, while the recognition effect for SFM, 2FSK, 4FSK and Frank code signals is slightly worse than that in [12]. The PSR of the method proposed in this paper is slightly lower than that in [12], because the method in [12] only needs to select the radar signal type with the highest recognition probability as the recognition result, while the method in this paper needs to determine not only the radar signal type, but also the number of radar signal components contained in the current pulse. Therefore, for the recognition system in this paper, even for the recognition of the single-component radar signal, its difficulty is no less than the recognition of the dual-component radar signal. The recognition effect of the recognition method in this paper for the single-component radar signal is not much different from that in [12]. Therefore, the method proposed in this paper is adaptable to the recognition of single-component signals.

## VII. CONCLUSION

In this paper, an intra-pulse modulation recognition approach for single-component and dual-component radar signals based on CNN and DQN is proposed. The approach can recognize the intra-pulse modulation modes of single-component radar signal and dual-component radar signal without knowing the number of signal components in the current signal. It can identify 8 typical types of intra-pulse modulation of the radar signal, including LFM, MP, SFM, BPSK, 2FSK, 4FSK, EQFM and Frank code. The simulation results show that the overall PSR of dual-component radar signals and single-component radar signals can reach 94.83% and 94.43%, respectively, when the SNR is  $-6$  dB. The results show that the proposed method can adapt to a lower SNR environment than the previous methods. It can be used to solve the wider problem of radar signal intra-pulse recognition in the radar reconnaissance system. However, the recognition effect of the proposed method depends on the training of a large number of data sets. How to design the network structure and obtain a recognition system with wide signal type adaptability based on limited data sets is a problem that needs to be solved in the future.

## REFERENCES

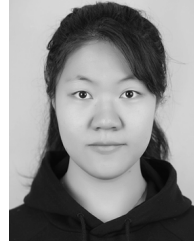
- [1] G. Latombe, E. Granger, and F. A. Dilkes, "Fast learning of grammar production probabilities in radar electronic support," *IEEE Trans. Aerosp. Electron. Syst.*, vol. 46, no. 3, pp. 1262–1289, Jul. 2010.
- [2] M. Gupta, G. Hareesh, and A. K. Mahla, "Electronic warfare: Issues and challenges for emitter classification," *Defence Sci. J.*, vol. 61, no. 3, pp. 228–234, 2011.
- [3] C. Shi, F. Wang, S. Salous, and J. Zhou, "Low probability of intercept-based radar waveform design for spectral coexistence of distributed multiple-radar and wireless communication systems in clutter," *Entropy*, vol. 20, no. 3, p. 197, 2018.
- [4] H. Yang and J. Chen, "Design of Costas/PSK continuous wave LPI radar signal," *Int. J. Electron.*, vol. 104, no. 3, pp. 404–415, Mar. 2017.
- [5] W. Lu, J. Xie, and H. Wang, "Parameterized time-frequency analysis to separate multi-radar signals," *J. Syst. Eng. Electron.*, vol. 28, no. 3, pp. 493–502, 2017.
- [6] T. Ravi Kishore and K. D. Rao, "Automatic intrapulse modulation classification of advanced LPI radar waveforms," *IEEE Trans. Aerosp. Electron. Syst.*, vol. 53, no. 2, pp. 901–914, Apr. 2017.
- [7] X. Ma, D. Liu, and Y. Shan, "Intra-pulse modulation recognition using short-time Ramanujan Fourier transform spectrogram," *EURASIP J. Adv. Signal Process.*, vol. 2017, no. 1, p. 42, Dec. 2017.
- [8] X. Fan, T. Li, and S. Su, "Intrapulse modulation type recognition for pulse compression radar signal," *J. Appl. Remote Sens.*, vol. 11, no. 3, Sep. 2017, Art. no. 035018.
- [9] M. Zhang, M. Diao, and L. Guo, "Convolutional neural networks for automatic cognitive radio waveform recognition," *IEEE Access*, vol. 5, pp. 11074–11082, 2017.
- [10] L. Gao, X. Zhang, J. Gao, and S. You, "Fusion image based radar signal feature extraction and modulation recognition," *IEEE Access*, vol. 7, pp. 13135–13148, 2019.
- [11] S.-H. Kong, M. Kim, L. M. Hoang, and E. Kim, "Automatic LPI radar waveform recognition using CNN," *IEEE Access*, vol. 6, pp. 4207–4219, 2018.
- [12] Z. Qu, X. Mao, and Z. Deng, "Radar signal intra-pulse modulation recognition based on convolutional neural network," *IEEE Access*, vol. 6, pp. 43874–43884, 2018.
- [13] Y. Yang, Z. Peng, X. Dong, W. Zhang, and D. A. Clifton, "Component isolation for multi-component signal analysis using a non-parametric Gaussian latent feature model," *Mech. Syst. Signal Process.*, vol. 103, pp. 368–380, Mar. 2018.
- [14] S. Chen, X. Dong, G. Xing, Z. Peng, W. Zhang, and G. Meng, "Separation of overlapped non-stationary signals by ridge path regrouping and intrinsic chirp component decomposition," *IEEE Sensors J.*, vol. 17, no. 18, pp. 5994–6005, Sep. 2017.
- [15] H. Zhu, S. Zhang, and H. Zhao, "Single-channel source separation of multi-component radar signal based on EVD and ICA," *Digit. Signal Process.*, vol. 57, pp. 93–105, Oct. 2016.
- [16] H. Zhu, S. Zhang, and H. Zhao, "Single-channel source separation of multi-component radar signal with the same generalized period using ICA," *Circuits, Syst., Signal Process.*, vol. 35, no. 1, pp. 353–363, Jan. 2016.
- [17] J. Gao, L. Shen, and L. Gao, "Modulation recognition for radar emitter signals based on convolutional neural network and fusion features," *Trans. Emerg. Telecommun. Technol.*, vol. 30, no. 12, Dec. 2019, Art. no. e3612.
- [18] J. Gao, L. Shen, L. Gao, and Y. Lu, "A rapid accurate recognition system for radar emitter signals," *Electronics*, vol. 8, no. 4, p. 463, 2019.
- [19] J. Wang, Y. Yang, J. Mao, Z. Huang, C. Huang, and W. Xu, "CNN-RNN: A unified framework for multi-label image classification," in *Proc. IEEE Conf. Comput. Vis. Pattern Recognit. (CVPR)*, Jun. 2016, pp. 2285–2294.
- [20] F. Lyu, Q. Wu, F. Hu, Q. Wu, and M. Tan, "Attend and imagine: Multi-label image classification with visual attention and recurrent neural networks," *IEEE Trans. Multimedia*, vol. 21, no. 8, pp. 1971–1981, Aug. 2019.
- [21] W.-J. Yu, Z.-D. Chen, X. Luo, W. Liu, and X.-S. Xu, "DELTA: A deep dual-stream network for multi-label image classification," *Pattern Recognit.*, vol. 91, pp. 322–331, Jul. 2019.
- [22] A. Krizhevsky, I. Sutskever, and G. E. Hinton, "ImageNet classification with deep convolutional neural networks," *Commun. ACM*, vol. 60, no. 6, pp. 84–90, May 2017.
- [23] K. He, X. Zhang, S. Ren, and J. Sun, "Deep residual learning for image recognition," in *Proc. IEEE Conf. Comput. Vis. Pattern Recognit. (CVPR)*, Jun. 2016, pp. 770–778.
- [24] V. Mnih, K. Kavukcuoglu, D. Silver, A. A. Rusu, J. Veness, M. G. Bellemare, A. Graves, M. Riedmiller, A. K. Fidjeland, G. Ostrovski, S. Petersen, C. Beattie, A. Sadik, I. Antonoglou, H. King, D. Kumaran, D. Wierstra, S. Legg, and D. Hassabis, "Human-level control through deep reinforcement learning," *Nature*, vol. 518, no. 7540, pp. 529–533, Feb. 2015.



**ZHIYU QU** received the Ph.D. degree in communication and information system from Harbin Engineering University, Heilongjiang, China, in 2008. In 2008, she joined the Nanjing Research Institute of Electronic Technology, where she has been studying in radar signal processing and passive target tracking. She is currently an Associate Professor with Harbin Engineering University. Her current research interests include wide band signals detection, high precision passive direction finding, and spatial spectrum estimation.

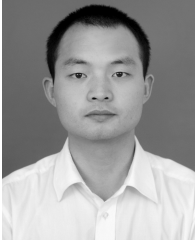


**CHENFAN HOU** received the bachelor's degree in electronics and information engineering from Harbin Engineering University, Heilongjiang, China, where he is currently pursuing the master's degree. His research interests include radar signal processing, machine learning, and image processing.



**WENYANG WANG** received the bachelor's degree in electronics and information engineering from Harbin Engineering University, Heilongjiang, China, where she is currently pursuing the master's degree. Her research interests include radar signal recognition, image processing, and machine learning.

...



**CHANGBO HOU** received the B.Eng. degree in communication engineering and the M.Eng. degree in communication and information system from Harbin Engineering University, Harbin, China, in 2008 and 2011, respectively. He is currently a Lecturer with the College of Information and Communication Engineering and the Doctor in Reading with the Key Laboratory of In-Fiber Integrated Optics, Ministry Education of China, Harbin Engineering University. His research interests include wideband signal processing and optical sensors.